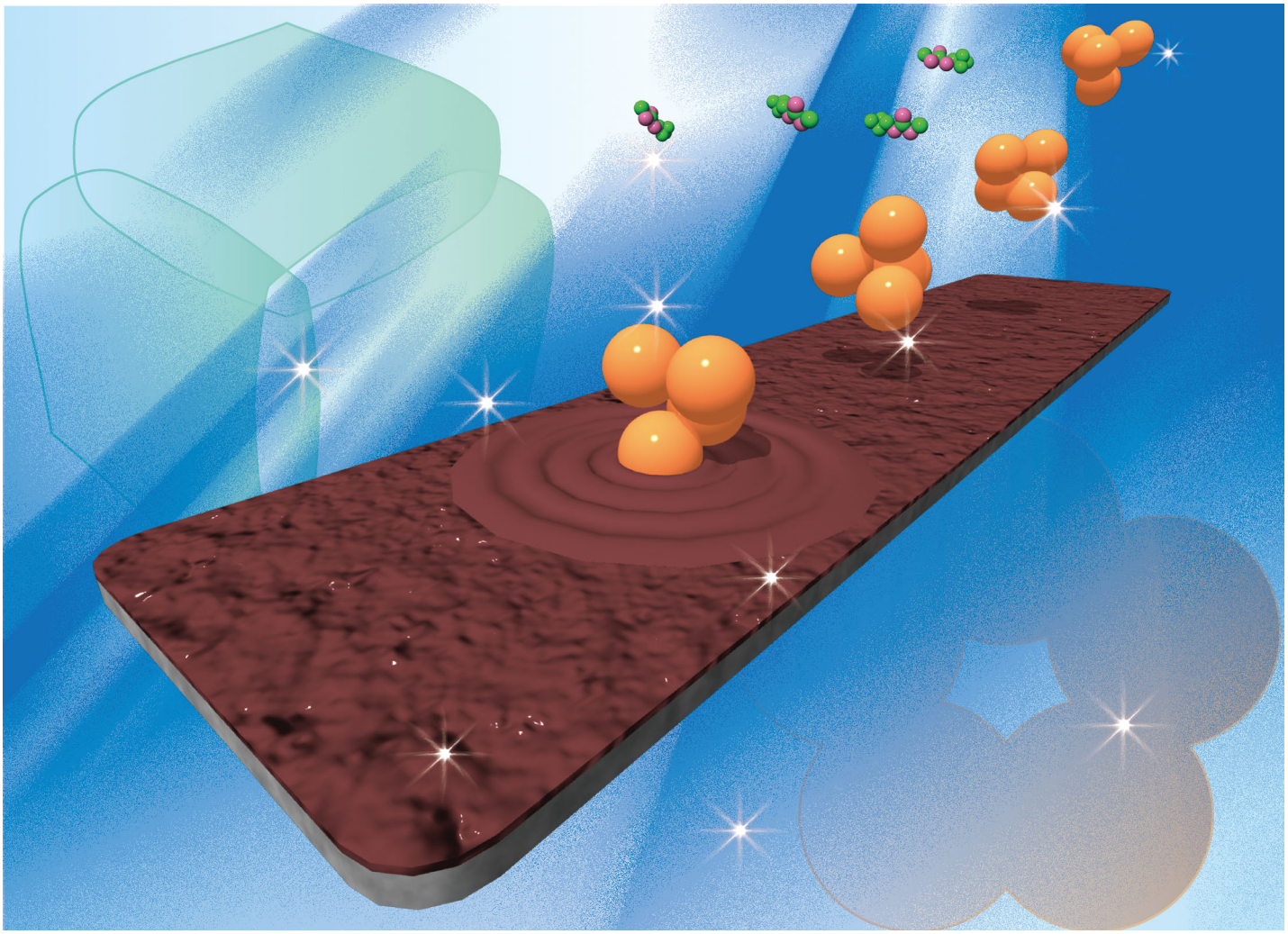
HOKKAIDO UNIVERSITY

Title	Use of decomposable polymer-coated submicron Cu particles with effective additive for production of highly conductive Cu films at low sintering temperature
Author(s)	Yong, Yingqiong; Mai Thanh Nguyen; Yonezawa, Tetsu et al.
Citation	Journal of materials chemistry C, 5(5), 1033-1041 https://doi.org/10.1039/c6tc04360g
Issue Date	2017
Doc URL	https://hdl.handle.net/2115/65126
Rights(URL)	https://creativecommons.org/licenses/by/3.0/
Type	journal article
File Information	c6tc04360g.pdf

Hokkaido University Collection of Scholarly and Academic Papers : HUSCAP

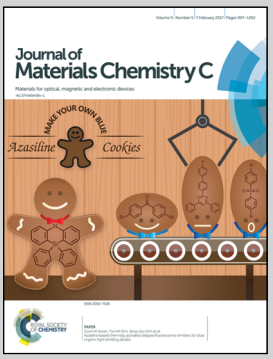


Showcasing international collaborative research from Division of Materials Science and Engineering, Faculty of Engineering, Hokkaido University; Criminal Investigation Laboratory, Tokyo Metropolitan Police Department; National Institute of Technology, Sendai College; and Department of Chemical Engineering, National Taiwan University.

Use of decomposable polymer-coated submicron Cu particles with effective additive for production of highly conductive Cu films at low sintering temperature

Decomposable polymer-coated copper fine particles and a self-reducible copper complex are used as an effective ink. This ink can be sintered at low temperature, *i.e.* 100 °C, to produce a highly conductive copper film.

As featured in:



See Tetsu Yonezawa *et al.*, *J. Mater. Chem. C*, 2017, **5**, 1033.

ROYAL SOCIETY OF CHEMISTRY

rsc.li/materials-c

Registered charity number: 207890

Journal of Materials Chemistry C

PAPER

View Article Online
View Journal | View Issue

Open Access Article. Published on 29 November 2016. Downloaded on 20/04/2017 06:52:53.
This article is licensed under a Creative Commons Attribution 3.0 Unported Licence.

Cite this: J. Mater. Chem. C, 2017, 5, 1033

Use of decomposable polymer-coated submicron Cu particles with effective additive for production of highly conductive Cu films at low sintering temperature†

Yingqiong Yong,[a] Mai Thanh Nguyen,[a] Tetsu Yonezawa,*[a] Takashi Asano,[ab] Masaki Matsubara,[ac] Hiroki Tsukamoto,[a] Ying-Chih Liao,[ad] Tengfei Zhang,[a] Shigehito Isobe[a] and Yuki Nakagawa[a]

Received 9th October 2016,
Accepted 28th November 2016

DOI: 10.1039/c6tc04360g

www.rsc.org/MaterialsC

A method for producing Cu films with low resistivity, based on low temperature sintering, is demonstrated. The Cu inks for preparing conductive Cu films consisted of Cu particles that were coated with a decomposable polymer (poly(propylenecarbonate), PPC) as well as a self-reducible copper formate/1-amino-2-propanol (CuF–IPA) complex as an additive. The sintering temperature used in this study was as low as 100 °C. Following sintering at a temperature of 100 °C, the lowest reported resistivity (8.8×10^{-7} Ω m) was achieved through the use of Cu-based metal–organic decomposition (MOD) inks. This was due to the dual promotional effects of the aminolysis of PPC with IPA and the pyrolysis of the CuF–IPA complex.

Introduction

Over the past few decades, conductive inks, used for printed electronics, have received increased attention.[1,2] They find application in various devices such as circuits,[3] light-emitting diodes (LEDs),[4] radio frequency identification (RFID) tags,[5] flexible displays,[6] and photovoltaics.[7]

Cu-based inks are an alternative printing material to noble metal nanoparticle inks owing to their low cost, low resistivity (1.7×10^{-8} Ω m, which is similar to that of silver) and high electromigration resistance. Fine Cu particles and nanoparticles[8] are stabilized using surfactants to prevent their oxidation.[9–11] Such stabilizers, which function as barriers, hinder the percolation paths of the Cu particles. This results in the production of printed patterns with high resistivity which are unsuitable for practical applications. Conventionally, in order to overcome this problem and to produce materials with good conductivity, high-temperature sintering (at 200 °C or higher) is performed using an oven under a designed atmosphere.[2,9–11] However, a much lower sintering temperature is necessary in the case of flexible and low-cost electronic devices that use heat-sensitive substrates, such as paper and polymeric substrates (*e.g.*, poly(ethylene terephthalate) (PET), polycarbonate (PC), polyethylene naphthalate (PEN)). Also, a low temperature sintering is indispensable for organic electronic assemblies. To reduce the sintering temperature, several approaches have been proposed; these include decreasing the particle size,[12,13] the use of Cu-based metal–organic decomposition (MOD) inks,[14–16] laser processes,[17–19] and photonic sintering.[20–22] Concerning the particle size reduction approach, reduction of particle size may lead to easier oxidation in the case of copper, which results in problems with storage. For laser sintering, Min *et al.* have used a copper complex as the ink. After drying the prepared film at 70 °C for 10 min, a laser sintering process was performed under nitrogen gas. The lowest resistivity they could obtain was 1.74×10^{-5} Ω cm by using a nanosecond-pulsed ultraviolet laser of 355 nm wavelength and 4.2 W maximum output power.[18] We have also used laser sintering for copper fine particle paste to generate electrically conductive copper film under a hydrogen/argon atmosphere. The films sintered under air showed insulating behaviour towards Cu_2O, but sintered

[a] Division of Materials Science and Engineering, Faculty of Engineering, Hokkaido University, Kita 13 Nishi 8, Kita-ku, Sapporo, Hokkaido 060-8628, Japan. E-mail: tetsu@eng.hokudai.ac.jp
[b] Criminal Investigation Laboratory, Tokyo Metropolitan Police Department, 2-2-1 Kasumigaseki, Chiyoda-ku, Tokyo, 100-8929, Japan
[c] Department of Materials and Environment Engineering, National Institute of Technology, Sendai College, 48 Nodayama, Medeshima-Shiote, Natori-shi, Miyagi 981-1239, Japan
[d] Department of Chemical Engineering, National Taiwan University, No. 1, Sec. 4, Roosevelt Rd., Taipei, 10617, Taiwan

† Electronic supplementary information (ESI) available: Synthesis and sintering of PPC-Cu inks; image and UV-Vis spectra of the CuF–IPA complex; TG/DTA-MS of CuF; TG/DTA of PPC; XRD patterns of the obtained Cu films sintered at 100 °C; SEM image of the obtained Cu films using PPC-Cu/CuF–IPA 2/3 inks sintered at 100 °C for 2 h; image of the PPC-Cu/CuF–IPA 2/1 ink; XRD patterns of PPC-Cu particles after sintering at 100 °C and 150 °C for 1 h and the resistivity of the obtained Cu films; SEM image of PPC-Cu particles after sintering at 100 °C for 1 h. See DOI: 10.1039/c6tc04360g

Open Access Article. Published on 29 November 2016. Downloaded on 20/04/2017 06:52:53.
This article is licensed under a Creative Commons Attribution 3.0 Unported Licence.

under H_2/Ar, the film with a high conductivity of 1.05×10^{-5} Ω cm was obtained.[19] Laser processes, however, are complex, low throughput, and associated with considerable environmental challenges.[23] Other methods have been studied for low temperature sintering such as photonic sintering of copper particles by Oh *et al.*[22] A low resistivity of 6–7 $\times 10^{-8}$ Ω m was achieved using photonic sintering at 2.5 kV for 1.5–2.0 ms. The substrate temperatures using such voltage were less than 110 °C. However, in the whole process, the preparation of copper nanoparticles required high temperature (150 °C) for a long time (*i.e.* 3 h) in nitrogen gas and prior to the photonic treatment, an hour ball milling and then air-brush printing process at 100 °C were also required. The produced copper nanoparticles were prone to oxidation. Moreover, photonic sintering requires high-intensity pulsed light (HIPL) irradiation equipment, which is expensive.[20,21] In contrast, MOD inks have been studied and used to produce films with high electrical conductivity *via* simple procedures. They consist of Cu salt, amine/amino hydroxyl ligands, and other organic components. In general, some organic components, such as diethyleneglycol methylether,[14] *n*-butanol,[14] ethyl cellulose,[24] 1-methyl-2-pyrrolidinone,[24] and octylamine,[25] are added to avoid the drawbacks associated with the use of only Cu salt and amine/amino hydroxyl ligands. Yabuki and coworkers have prepared the MOD ink using copper(II) formate (CuF) and various amines. After sintering at 130 and 140 °C using copper and blended amines of octylamine and dibutylamine, the resistivity could reach the order of magnitude of 10^{-8} Ω m (140 °C, 5×10^{-8} Ω m). On lowering the sintering temperature to 110 °C, it was observed that the produced copper film had the resistivity being increased by one order of magnitude (*i.e.* 10^{-7} Ω m) by using the copper–octylamine complex.[16] Our group has proposed for the first time to replace these organic components through the addition of highly conductive, submicron Cu particles. As a result, following sintering at a temperature of 100 °C, a conductive Cu film, with a low resistivity of 9.0×10^{-6} Ω m, was obtained.[15] In the case of inks that used a Cu complex with fine Cu particles, the sintering temperature required to achieve low resistivity (in the range of 10^{-6} to 10^{-8} Ω m) was lower compared to that of the inks that used a Cu complex with other organic components.[14,16,24–26] This was because the added Cu particles were highly conductive and also directly contributed to the higher packing density of the sintered Cu films.[15] Recently, Suganuma's group has prepared CuF and 2-amino-2-methyl-1-propanol together with copper seeds as the ink for conductive copper film. After heating at 120 and 140 °C for 15 min, they achieved resistivities of 6×10^{-7} and 1×10^{-7} Ω m, respectively.[27] Further investigation is needed in using this method for a lower sintering temperature.

In addition, researchers have also focused on the surface modification of metal nanoparticles to promote particle sintering at a low temperature. Magadassi and co-workers triggered the sintering of silver nanoparticles by charge neutralization or desorption of the stabilizer.[28] Long *et al.* achieved rapid sintering of silver nanoparticles *via* the formation of ion pairs between the cations of the electrolyte and the benzoquinone with a π-conjugated system, which presented as radical anions on the particle surface. The formation of ion pairs weakened the interaction between the silver atoms at the surface and the benzoquinone, consequently reducing their stability; this caused the silver nanoparticles to coalesce at room temperature.[29] Grouchko and co-workers used a built-in sintering mechanism, where a destabilizing agent was used to detach the anchoring groups of the stabilizer from the surface of the particle. This enabled coalescence and sintering of the silver particles at room temperature.[30]

By mixing commercial submicron Cu particles with a Cu complex, our group has produced Cu films with low resistivity (9.0×10^{-6} Ω m) at low sintering temperature (100 °C) under nitrogen.[15] However, in this study, commercially available copper particles were applied as materials for sintering and no surface modification was performed. It is known that surface modification and stabilizing organic reagents strongly affect the sintering behaviour of metal particles. Therefore, to further reduce the resistivity of films sintered at low temperature, smaller Cu particles coated with an amine-assisted decomposable polymer (polypropylene carbonate, PPC) were used as a new component in Cu-based MOD inks, where the other components were copper formate (CuF) and 1-amino-2-propanol (IPA). The use of smaller Cu particles with a wider size distribution could improve the stability of the inks, and denser sintered copper films were obtained. Moreover, PPC, used as the capping agent of the added Cu particles, could break down into smaller molecules *via* an aminolysis reaction with IPA. Previously, we have used a proton-initiated degradable polymer for stabilizing fine copper particles for a low temperature sintering.[31] This polymer contains ether bonds in the main chain and can be decomposed at low temperature in the presence of protons. In the presence of formic acid, electro-conductive films with low resistivity were obtained at temperatures as low as 150 °C. Usage of degradable polymers is one of the important factors to make the sintering temperature lower. Degradation of the stabilizing polymer molecules could consequently trigger the coalescence and sintering of the added particles as well as the Cu particles generated from the pyrolysis of CuF. However, we noted that without decomposition of the CuF–IPA complex and using only proton decomposable polymer coated copper particles for the preparation of the ink, hot-pressing or sintering under reducing gas (3% H_2/N_2) at 150 °C is required for obtaining low resistivity.[31]

In the present study, therefore, we modified the surface of copper particles with an amine-decomposable polymer and used the mixture of these copper particles and the CuF–IPA complex as the ink for achieving low resistivity at low sintering temperature (100 °C) under nitrogen gas. We demonstrate that the Cu films that were sintered at low temperature had low resistivity because of the synergistic effects arising from the presence of the decomposable polymer-coated Cu particles with a wide size distribution and the CuF–IPA additive. Under a nitrogen atmosphere, without the use of a reductive gas (*e.g.*, hydrogen or formic gas), a Cu film with a resistivity of 8.8×10^{-7} Ω m was produced using a sintering temperature of 100 °C.

Experimental section

Preparation of PPC-stabilized fine Cu particles (PPC-Cu)

First, 3.6 g of PPC (Sumitomo Seika Chemicals Co., Japan, M_w = 248 000, measured by GPC in terms of polystyrene) was

 This journal is © The Royal Society of Chemistry 2017

Open Access Article. Published on 29 November 2016. Downloaded on 20/04/2017 06:52:53.
This article is licensed under a Creative Commons Attribution 3.0 Unported Licence.

dissolved in 180 cm^3 of tetrahydrofuran (THF, Kanto). Subsequently, 3.6 g of cupric oxide (CuO) micro-particle agglomerates (Nissin Chemco, Japan), with sizes ranging from a few hundred nanometers to several micrometers, was added into the above solution and heated to 60 °C and stirred at a speed of 433 rpm. Then, 10.8 cm^3 of hydrazine monohydrate (Junsei) was introduced into the mixture, whereupon an instant colour change, from black to brown-red, occurred. This dispersion was heated for 1 h. Following the reaction, the dispersion was subjected to centrifugation three times, with ethanol and ethyl acetate, and was subsequently dried under a nitrogen atmosphere; finally, PPC-capped Cu particles were obtained.

Preparation of PPC-stabilized Cu particles/$Cu(HCOO)_2$–IPA (1-amino-2-propanol) mixed inks (PPC-Cu/CuF–IPA) and sintered Cu films

CuF–IPA complexes were prepared by mixing equal moles of copper(II) formate tetrahydrate (CuF, $Cu(HCOO)_2{\cdot}4H_2O$, Wako) and 1-amino-2-propanol (IPA, Junsei) using a conditioning mixer for 40 min. IPA was selected in this study because CuF–IPA complexes kept their liquid form without generating any solid compounds for more than 2 weeks.[15] The synthesized PPC-stabilized fine Cu particles were added into the CuF–IPA complex and mixed for 16 min using a conditioning mixer to form PPC-Cu/CuF–IPA inks. The detailed compositions of the inks are given in Table 1. For all the inks, the total amount of CuF, IPA, and Cu atoms in the PPC-Cu particles was 16 mmol. Inks with molar ratios of 6/1, 2/1, and 2/3 (Cu mol of PPC-Cu/Cu mol of CuF–IPA) were prepared; the CuF and IPA in the Cu inks were equimolar. The inks were denoted using the molar ratios, and the sintered films were prepared from the corresponding inks. The inks were then printed on the Al_2O_3 substrate, to a thickness of 40 μm, using a doctor blade. Subsequently, the printed films were sintered at 100 °C under a nitrogen atmosphere for various periods. The heating speed in the sintering process was 10 °C min^{-1} from room temperature to 90 °C and 1 °C min^{-1} from 90 °C to 100 °C. Nitrogen gas was provided from a cylinder and the purity was 99.99%. No reductive gas was used during sintering.

Characterization

X-ray diffraction (XRD) patterns were obtained using a Rigaku Miniflex-II diffractometer. Scanning electron microscopy (SEM) images of the PPC-Cu particles and Cu films were obtained using a JEOL JSM-6701F field-emission-type SEM. Thermogravimetric differential thermal analysis (TG-DTA) was performed using a Shimadzu DTG-60H. The decomposition of the CuF and CuF–IPA complex was analyzed using thermal desorption mass spectrometry measurements (TDMS, Ulvac, BGM-102) combined with thermogravimetry and differential thermal analyses (TG-DTA, Bruker, 2000SA). The resistivity of the Cu films was measured *via* a four-point probe method using a Mitsubishi Chemical Analytech Loresta-GP with an ASP probe. UV-Vis spectra were obtained using a Shimadzu UV-1800. To prepare the samples for UV-Vis measurements, ethanol was used as a solvent to dissolve the CuF–IPA complex (1 wt% CuF–IPA complex in ethanol). A Fourier transform infrared spectrometer (FTIR, Jasco FT/IR-4600) was used to produce the FTIR spectra of the samples. Matrix-assisted laser desorption ionization mass spectroscopy (MALDI-MS) data were recorded using an Autoflex speed (Bruker Daltonics, 335 nm laser (laser power = 50, this is a control parameter of the instrument) was used for desorption/ionization) to elucidate the decomposition of the PPC with an amino group. Positive reflectron mode was selected. The data of 10 000 shots (2000 shots × 5 spots) were accumulated to obtain a spectrum. The mass spectrum of the original PPC could not be obtained as its mass exceeded the mass range of the spectrometer. PPC + IPA following heating at 100 °C for 3 h under a nitrogen atmosphere (weight ratio, PPC : IPA = 1 : 1) was dissolved in 9 cm^3 of acetonitrile to prepare the MALDI-MS samples. α-Cyano-4-hydroxycinnamic acid (CHCA) was selected as the matrix. CHCA was dissolved in acetonitrile (5 mg cm^{-3}) with the addition of 0.1% tetrafluoroacetic acid (TFA). After mixing the same volume of the sample and the CHCA solution, 1 mm^3 of mixed solution was added to the sample well. The sample was dried under ambient conditions before measurement.

Table 1 Sample names and the corresponding compositions of the inks

Sample name	Composition of ink		
PPC-Cu/CuF–IPA	Cu atoms in PPC-Cu particles/mmol	CuF/mmol	IPA/mmol
6/1	12	2	2
2/1	8	4	4
2/3	4	6	6

CuF: copper(II) formate, IPA: 1-amino-2-propanol.

Results and discussion

Preparation and characterization of fine PPC-Cu particles

The fine PPC-Cu particles were synthesized using hydrazine as a reducing agent of CuO microparticles at a low reaction temperature of 60 °C under an ambient atmosphere. Fig. 1a shows a SEM image of the obtained PPC-Cu particles. The size

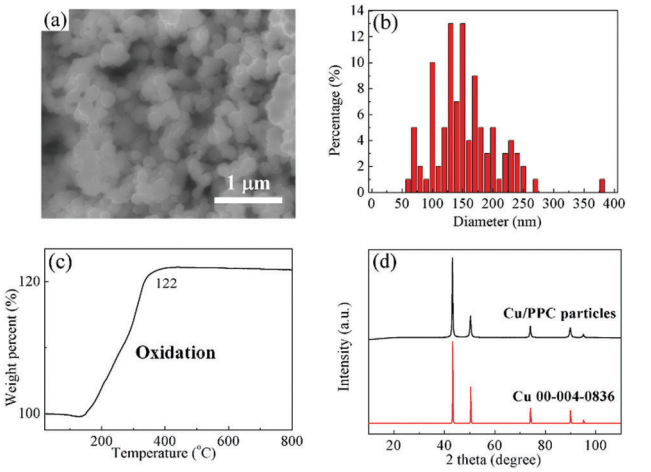


Fig. 1 (a) SEM image, (b) size distribution, (c) TG result for heating in air, and (d) XRD pattern of the fine PPC-Cu particles.

Open Access Article. Published on 29 November 2016. Downloaded on 20/04/2017 06:52:53.
This article is licensed under a Creative Commons Attribution 3.0 Unported Licence.

of the PPC-Cu particles was 154 ± 54 nm as shown in Fig. 1b. The wide size distribution of the particles facilitated the formation of a well-packed particulate structure as well as the low temperature sintering. Following sintering, the packing density of the obtained Cu films increased because the voids between the large particles were filled with small particles; this resulted in good conductivity.[32] The TG results (Fig. 1c) reveal that the amount of PPC in the fine PPC-Cu particles was 2.2 wt%. The amount of PPC in PPC-Cu was calculated from the initial mass of PPC-Cu and the mass of the final product, CuO, obtained after heating PPC-Cu to 600 °C in air to burn out PPC and completely oxidize Cu. From the mass of CuO, the mass of Cu in PPC-Cu can be calculated, and thereby the mass of PPC in Cu-PPC can be obtained. In the XRD pattern (Fig. 1d), no Cu oxide peaks (Cu_2O, CuO, or other metastable phases[33–35]) can be observed and all the peaks are identical to that of the reference pattern of Cu, indicating that the Cu particles were effectively protected by PPC.

Decomposition of the CuF–IPA complex

The prepared CuF–IPA complex consisted of a blue liquid with a relatively high viscosity (Fig. S1, ESI†). IPA can have bidentate interactions with Cu to form stable five-membered metallacycle structures according to the hard soft acid base theory.[14] The CuF–IPA complexes, produced using various mixing times, were investigated using UV-Vis spectroscopy (Fig. S2, ESI†). The spectroscopic results indicate that no obvious red/blue shift of the extinction peaks occurred, demonstrating that there was negligible change in the ligand-field intensity when the mixing time was varied from 24 min to 56 min.[36] In this work, a mixing time of 40 min was selected to prepare the CuF–IPA complex.

The self-redox reaction of CuF generates Cu and volatile products (H_2, CO_2), as shown in eqn (1)–(3):

$$Cu(HCOO)_2 \rightarrow Cu(HCOO) + 1/2H_2(g) + CO_2(g) \quad (1)$$

$$Cu(HCOO) \rightarrow Cu(s) + 1/2H_2(g) + CO_2(g) \quad (2)$$

In total:

$$Cu(HCOO)_2 \rightarrow Cu(s) + H_2(g) + 2CO_2(g) \quad (3)$$

IPA can also function as a reducing agent. It was reported that the secondary OH group of IPA can partly reduce Cu oxide to metallic Cu under a nitrogen atmosphere.[12]

This process was investigated using TGA (Fig. 2) and DTA/TGA-MS (Fig. 3 and Fig. S3, ESI†). Compared with the self-reduction of CuF, the reduction of the CuF–IPA complex, to form Cu, can commence at lower temperature and be accelerated because of the presence of IPA, which acts as a reducing agent. The complete decomposition temperature of the CuF–IPA complex (141 °C) was ~95 °C lower than that of CuF (236 °C), as shown in Fig. 2. In the case of CuF, the release of a large quantity of bound water and CO_2, due to the decomposition of CuF, was detected between 183 °C and 236 °C, which corresponds with the weight loss observed in Fig. 2 and the endothermic peak in Fig. S3 (ESI†). In contrast, the decomposition process of the CuF–IPA complex was more complicated.

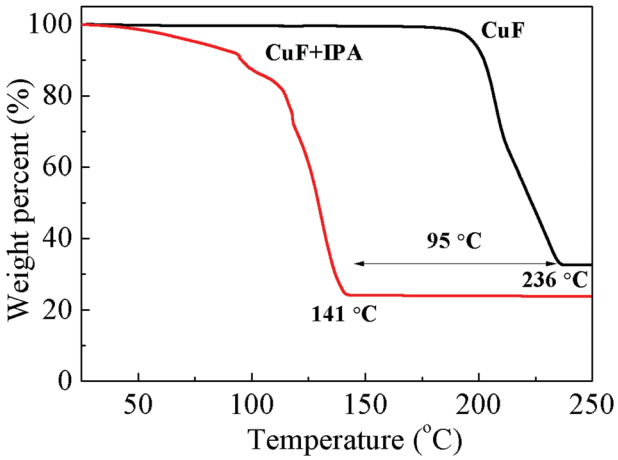


Fig. 2 TGA curves of CuF and CuF–IPA complexes (CuF : IPA = 1 : 1, mol/mol) under He gas.

The DTA/TGA-MS data of CuF–IPA were recorded, and are shown in Fig. 3. The main gaseous products of this process are shown in Fig. 3b and c as a function of temperature. The non-bound water evaporated and a small amount of CO_2 was generated at approximately 100 °C (Fig. 3c). The generation of CO_2 at around 100 °C indicates the partial decomposition of CuF to the lower valence states of Cu (eqn (1)–(3)). A large quantity of Cu(II) was reduced to Cu(I) (eqn (1)), and was accompanied by the release of formate, C, CO_2, and fragments of IPA (exothermic peaks at 118 °C). Two exothermic DTA peaks can be observed at 125 and 128 °C (Fig. 3d). During this process, Cu(I) was further reduced to Cu(0) and a second formate was released as CO_2 (eqn (2)). In addition, C, formate, and fragments of IPA evaporated. The endothermic peak at 133 °C was related to the evaporation of the bound water, CO_2, and fragments of IPA.

In summary, the results confirm that the decomposition of the CuF–IPA complex, to Cu, commenced at ~100 °C and ended at ~143 °C.

Merits of PPC-stabilized fine Cu particles and Cu film formation with PPC-Cu/CuF–IPA

In our previous study, we demonstrated that the use of mixed inks containing a Cu complex and commercially available submicron Cu particles (~0.8 μm) increased the uniformity and packing density of the obtained Cu films. The films, produced at a low sintering temperature of 100 °C, had high conductivity.[15] This was ascribed to the increased contacts between the added Cu particles and the Cu generated by the pyrolysis of CuF. The use of smaller Cu particles with a wide size distribution is favorable for further improving the conductivity of the Cu films sintered at low temperature. However, organic stabilizers are usually required to control the size of the particles as well as prevent surface oxidation.[35] These organic stabilizers obstruct contacts between the particles and limit the number of electron percolation paths, resulting in low conductivity (high resistivity). In general, the use of a higher sintering temperature is required for the removal of the organic layers.[9–11]

 This journal is © The Royal Society of Chemistry 2017

Open Access Article. Published on 29 November 2016. Downloaded on 20/04/2017 06:52:53.
This article is licensed under a Creative Commons Attribution 3.0 Unported Licence.

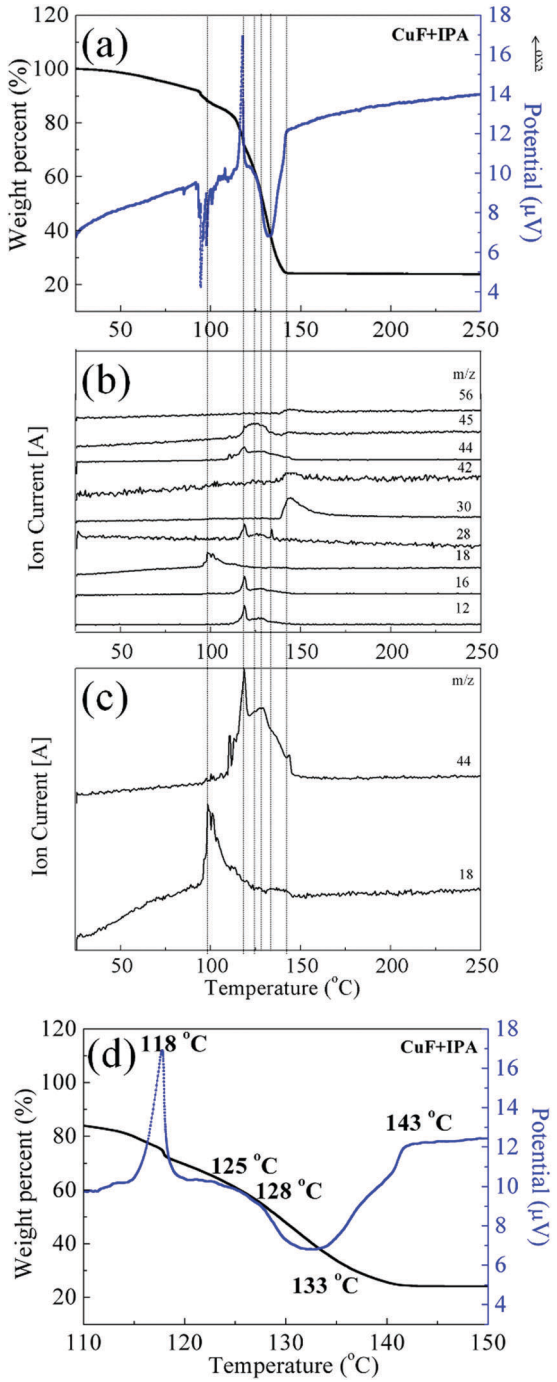


Fig. 3 TG/DTA-MS of the CuF–IPA complex (CuF : IPA = 1 : 1, mol/mol) under He gas: (a) DTA/TGA data, (b) fragments obtained at different temperatures, detected by MS (mass to charge ratio (*m*/*z*) *versus* temperature), (c) magnification of spectra shown in (b) for *m*/*z* of 44 and 18, (d) TG/DTA data of the CuF–IPA complex from 110 to 150 °C. The main pyrolysis products and their fragments determined based on the mass to charge ratios (*m*/*z*) were C (amu = 12), CH_4 (amu = 16), H_2O (amu = 18), CO or CH_2CH_2 (amu = 28), CH_4N (amu = 30), CH_3CHCH_2 (amu = 42), CO_2 (amu = 44), HCOO (amu = 45), and $(CH_2)_2CO$ (amu = 56).

In this work, to exploit the use of smaller Cu particles with a wide size distribution and to avoid the use of high sintering temperatures for the removal of the organic stabilizers, an amino-induced decomposable polymer, PPC, was selected as a capping agent for the fine Cu particles. PPC is a biodegradable and biocompatible polymer. PPC is an alternating copolymer of carbon dioxide (~43% of total weight) and propylene oxide (PO). It can be used to reduce white pollution in the environment.[37–39] PPC can decompose at 200–250 °C (Fig. S4, ESI†), but its decomposition temperature can be lowered *via* an aminolysis reaction with amine or amino alcohol (Fig. 4).[40] The aminolysis results in a reduction of the effective steric stabilization of the particles and facilitates the coalescence and sintering of the particles.

In this work, we studied the effects of the fine PPC-Cu particles on the resistivity of the Cu films. Fig. 5 shows the resistivities of the Cu films following sintering for 1 h at 100 °C under a nitrogen atmosphere; various PPC-Cu/CuF–IPA mixed inks were used (Table 1). The resistivities of the films obtained using the PPC-Cu/CuF–IPA (6/1, 2/1, and 2/3) inks were 1.5×10^{-6}, 8.8×10^{-7}, and 2.4×10^{-6} Ω m, respectively. The Cu films prepared using the lowest and the highest quantities of PPC-Cu particles, the PPC-Cu/CuF–IPA 2/3 and 6/1 inks, respectively, had resistivities that were 2–3 times that of the Cu film produced using the PPC-Cu/CuF–IPA 2/1 ink. To elucidate the underlying reason for this result, we investigated the structure and morphology of the sintered Cu films.

Following sintering for 1 h, all the Cu films were formed without any oxides, as shown by the XRD results (Fig. S5, ESI†). This is owing to the self-redox reaction of CuF, which releases hydrogen gas, enhancing the reducing atmosphere. In addition, the decomposition of CuF–IPA releases IPA molecules, which can also contribute to the reducing environment that surrounds

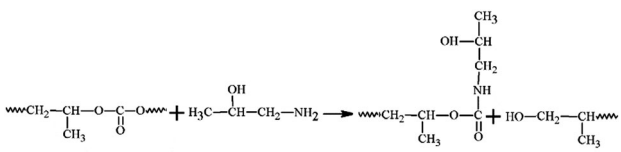


Fig. 4 The aminolysis of PPC with IPA.

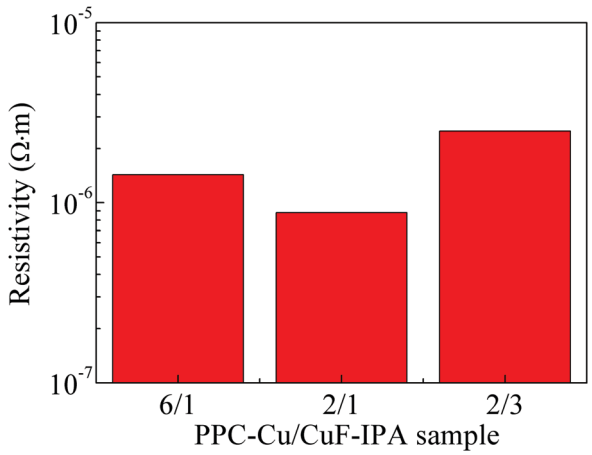


Fig. 5 Resistivities of the Cu films obtained using Cu inks, as shown in Table 1, following sintering at 100 °C for 1 h under a N_2 gas.

Open Access Article. Published on 29 November 2016. Downloaded on 20/04/2017 06:52:53.
This article is licensed under a Creative Commons Attribution 3.0 Unported Licence.

the Cu particles. Considering the particle size after sintering (shown later), which is larger than 100 nm, the oxidation can be negligible. Only very small part of the particle surface may be partially oxidized to $Cu_{64}O$ or Cu_2O.[35]

Fig. 6 presents the SEM images and the corresponding size distributions of the Cu films obtained following sintering for 1 h. In all cases, the Cu particles are larger than the fine PPC-Cu particles (154 ± 54 nm) used in the inks. They could be formed as a result of sintered products of the PPC-Cu particles and Cu particles generated by the pyrolysis of CuF. The particle size of the sintered Cu films increased when fewer fine PPC-Cu particles and a greater quantity of CuF–IPA were used in the inks. Moreover, when the sintering time was increased from 1 to 2 h, there was a significant decrease in the resistivity of the sintered Cu films containing the lowest quantity of fine PPC-Cu particles. However, no obvious changes were observed for the other films that contained a greater quantity of fine PPC-Cu particles (Table 2). In the case of the Cu film containing the lowest quantity of fine PPC-Cu particles that was obtained by sintering for 2 h, the particles were more tightly packed and had more contacts with each other (Fig. S6, ESI†) compared with those of the Cu film that was sintered for 1 h (Fig. 6c) (closer particle contacts can increase the number of percolation paths as well as the packing density, which consequently results in higher conductivity). In the case of Cu film containing the lowest quantity of the fine PPC-Cu particles, the Cu particle size after 1 h sintering was more than 50 nm. According to Gibbs–Thomson equation which expresses the relationship between particle size and melting point, it is impossible to enhance the melting of large nanoparticles (*e.g.* 50 nm) at 100 °C by another 1 h heating.[1,41] The possible reason for the decrease of resistivity from 1 h to 2 h sintering was the further improvement in the contact among Cu particles by the generated Cu particles from the complete pyrolysis of CuF or the further sintering of the small Cu nanoparticles that existed in the film after the previous 1 h heating. The Cu films prepared from the ink containing the largest quantity of PPC-Cu particles (PPC-Cu/CuF–IPA 6/1 ink) exhibited high resistivity (Fig. 5 and Table 2). This can be ascribed to the large quantity of the PPC stabilizer. Any excess PPC that was not completely decomposed by the IPA in the ink could inhibit contacts between the Cu particles and decrease the conductivity of the Cu films. Based on the above analysis, it can be determined that the PPC-Cu/CuF–IPA 2/1 ink (Fig. S7, ESI†) had the optimal composition, containing sufficient PPC-Cu, CuF, and IPA for the production of Cu films with low resistivity (8.8×10^{-7} Ω m) at a low sintering temperature (100 °C) and a short sintering time (1 h). The schematic representation in Fig. 7 can be used for explaining the above results. The decomposition of PPC with IPA during sintering at 100 °C will be also demonstrated and discussed in the paper.

When using the PPC-Cu/CuF–IPA 2/1 ink with the optimal composition, optimization of the sintering time was discussed. When the sintering periods were 15 and 30 min, the resistivities of the Cu films were beyond the measurement range. Many organics were present and there were no contacts between the particles, as shown in the SEM images (Fig. 8a and b). The reduction of CuF was not complete, and the short sintering time was insufficient for the PPC to decompose. In addition, the images of the films obtained following sintering for 1 and 2 h show the presence of Cu particles that are highly packed (Fig. 8c and d). Following sintering for 1 and 2 h, the resistivities were 8.8×10^{-7} and 10.0×10^{-7} Ω m, respectively. There was no obvious change in the resistivity when the sintering time was extended beyond 1 h. Therefore, 1 h was determined to be the optimal sintering time.

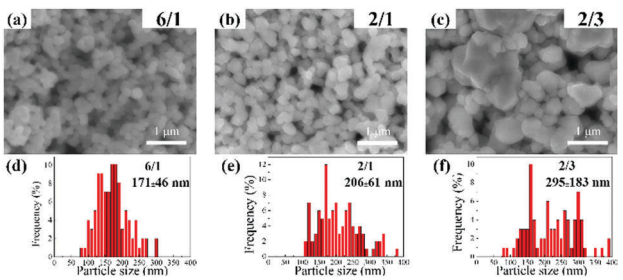


Fig. 6 SEM images (a, b, and c) and the corresponding size distributions (d, e, and f) of the Cu films obtained after sintering at 100 °C for 1 h, using (a and d) PPC-Cu/CuF–IPA 6/1, (b and e) PPC-Cu/CuF–IPA 2/1 and (c and f) PPC-Cu/CuF–IPA 2/3 mixed inks.

Table 2 The resistivities of Cu films obtained by sintering under N_2 for various periods

Sample	Sintering time at 100 °C/h	Resistivity/ $\times 10^{-7}$ Ω m
PPC-Cu/CuF–IPA 6/1	1	15.0
	2	18.0
PPC-Cu/CuF–IPA 2/1	1	8.8
	2	10.0
PPC-Cu/CuF–IPA 2/3	1	24.0
	2	10.0

Aminolysis of PPC with IPA at 100 °C

From the above results and discussion, it is obvious that the decomposition of PPC at low sintering temperature is crucial for obtaining sintered Cu films with low resistivities. During the sintering process (Fig. 9), PPC breaks down into small

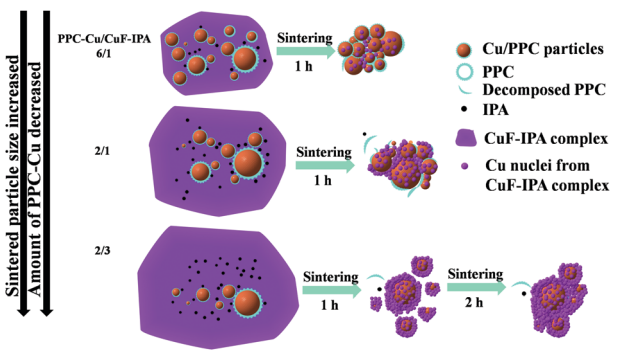


Fig. 7 Schematic representation of the sintering process for various PPC-Cu/CuF–IPA mixed inks.

This journal is © The Royal Society of Chemistry 2017

Open Access Article. Published on 29 November 2016. Downloaded on 20/04/2017 06:52:53.
This article is licensed under a Creative Commons Attribution 3.0 Unported Licence.

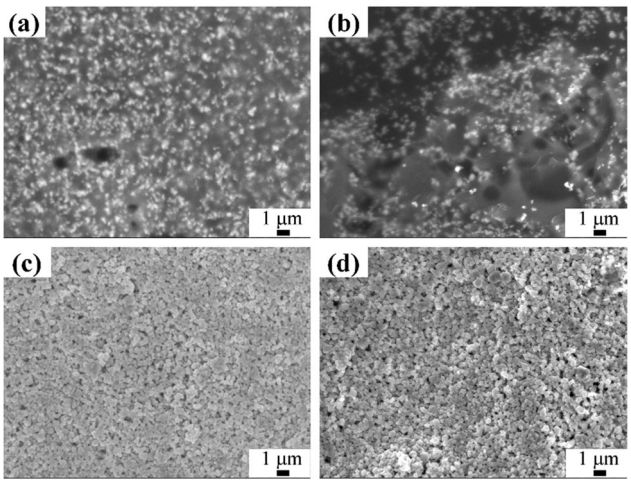


Fig. 8 SEM images of obtained Cu films following sintering at 100 °C for (a) 15 min, (b) 30 min, (c) 1 h, and (d) 2 h using the PPC-Cu/CuF–IPA 2/1 ink.

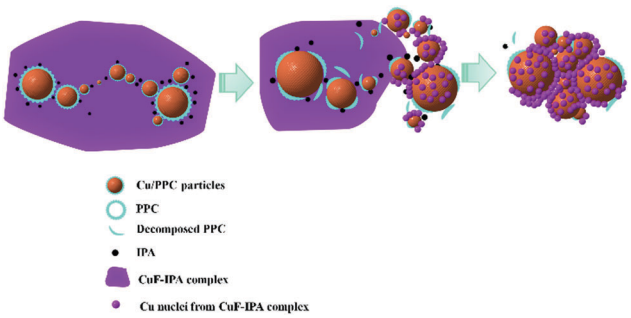


Fig. 9 Scheme of the sintering process.

molecules as a result of aminolysis with IPA (Fig. 4); this facilitates particle coalescence and sintering, and also decreases the resistivity. To confirm that the aminolysis process occurred during sintering at 100 °C, FT-IR was performed to detect the formation of the amide group from the reaction between the amino group of IPA and the carboxyl group of PPC. Fig. 10 shows the FT-IR spectra, in the range of 500–4000 cm^{-1}, of PPC, IPA, and PPC + IPA at room temperature, and that of PPC and PPC + IPA following heating at 100 °C for 3 h under a nitrogen atmosphere. Following heating at 100 °C, the IR spectrum of PPC was identical to that of PPC at room temperature (Fig. 10). The FTIR spectrum of the PPC and IPA mixture without heating was equivalent to the sum of the individual PPC and IPA spectra. In contrast, in the case of the PPC and IPA mixture that was heated at 100 °C, three obvious absorbance peaks could be observed for the amide group; these were 3300–3250 cm^{-1} (N–H stretching of secondary amide), 1680–1640 cm^{-1} (C═O stretching of the amide II band) and 1560–1530 cm^{-1} (coupling of N–H bending and C–N stretching of the amide II band).[42] In the range of 3300–3250 cm^{-1}, besides N–H stretching we do not exclude the possible contribution of the O–H group (in IPA or hydrolysis products). The above results demonstrate that the aminolysis of PPC occurred during the sintering at 100 °C. On the other hand, the presence of organic residuals (*e.g.* amide) as evident in FTIR

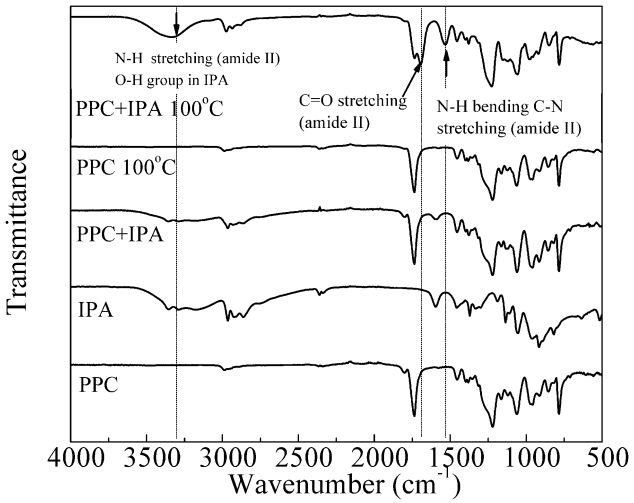


Fig. 10 FTIR spectra of PPC, IPA, and PPC + IPA (weight ratio, PPC : IPA = 1 : 1) at room temperature, and PPC and PPC + IPA (weight ratio, PPC : IPA = 1 : 1) following heating at 100 °C for 3 h under N_2.

is important because they can enhance the adhesion of the metal film to the substrate, especially when an organic substrate is used. Sugiyama *et al.*[13] have reported that the organic capping agent formed a residue to enhance the adhesion of the formed film to the polyimide substrate.

MALDI-MS measurements were carried out with the original PPC molecules and the degraded components after aminolysis in the presence of IPA. The molecular weight of the original PPC measured by GPC was 248 000 (in terms of polystyrene) which is larger than the mass range which can be measured by the spectrometer and we could not obtain its mass spectrum by MALDI-MS. Fig. 11 shows the MALDI mass spectrum of PPC molecules after aminolysis in the presence of IPA molecules. Strong mass peaks with constant mass intervals of 102, which correspond to $C_4H_6O_3$ (102 Da, see inset), can be found in the

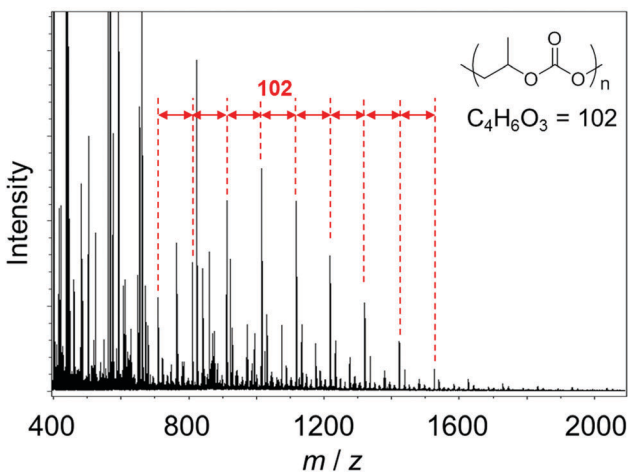


Fig. 11 MALDI mass spectrum of PPC molecules after aminolysis in the presence of IPA. Clear strong peaks are observed with a constant mass interval of 102. The molecular weight of the original PPC was M_W = 248 000 (measured by GPC; MALDI-MS could not show the peaks because the mass of the original PPC exceeded the measurement range).

Open Access Article. Published on 29 November 2016. Downloaded on 20/04/2017 06:52:53.
This article is licensed under a Creative Commons Attribution 3.0 Unported Licence.



m/z range between 600 and 1600. These peaks clearly indicate that PPC molecules were degraded in the presence of IPA at 100 °C by aminolysis. This degradation should help the low temperature sintering of our PPC-stabilized fine copper particles.

To further confirm the effectiveness of the CuF–IPA complex and PPC-Cu particle mixture on the resistivity, only the PPC-Cu particles were sintered under a nitrogen atmosphere (detailed preparation method in ESI†). The XRD patterns of the sintered PPC-Cu particles exhibit signals that can be attributed to Cu, without any evidence of the existence of Cu oxides (Fig. S8, ESI†). Noticeably, the resistivities of the Cu films using only PPC-Cu particles that were sintered at 100 and 150 °C were beyond the measurement range (Table S1, ESI†). Following sintering at 100 °C, the resistivity of the Cu film using only PPC-Cu particles was much higher than that of the sintered Cu films using the PPC-Cu/CuF–IPA inks (Table 2). There was much less contact between the particles in the sintered film that used only PPC-Cu particles (Fig. S9, ESI†) compared with that of the sintered films that used the PPC-Cu/CuF–IPA inks (Fig. 6). This is consistent with the resistivity measurement results.

For the first time, we modified the surface of copper particles with the PPC polymer which can be decomposed easily in the presence of an amine and used the mixture of these copper particles and the CuF–IPA complex as the ink for achieving low resistivity at low sintering temperature (100 °C). We demonstrated that the decomposition of the coating polymer in the sintering process of the ink is important for achieving low temperature sintering with low resistivity. Our method using MOD inks offers a simple procedure and low temperature thermal sintering in N_2 offers low cost. We believe that our method makes sintering of copper conductive inks for low-cost electronic devices closer to practical application.

Conclusions

In this work, to achieve effective sintering of Cu films at 100 °C, decomposable polymer (PPC)-coated Cu particles, with a size distribution of 154 ± 54 nm, were used to prepare PPC-Cu/CuF–IPA inks. We have demonstrated that the aminolysis of PPC with IPA effectively enhanced the conductivity of the sintered Cu films. The PPC-Cu particles with a smaller size and a wide size distribution were beneficial for increasing the packing density of the sintered Cu films due to less vacancy between particles after sintering. In addition, Cu particles obtained from the pyrolysis of CuF could also increase contacts between particles by deposition on the surface of PPC-Cu or filling in the space between PPC-Cu particles. This led to the production of Cu films with higher conductivity. With the aforementioned dual promotional effects, the lowest reported resistivity (8.8×10^{-7} Ω m) at a sintering temperature of 100 °C was achieved using Cu-based MOD inks.

Acknowledgements

The authors are grateful for the fruitful discussions with Mr N. Fujimoto (Sumitomo Seika), Dr Y. Ishida (Hokkaido Univ.) and Mr K.-M. Huang (National Taiwan University). This work is partially supported by Canon Foundation. MTN and TY thank Hokkaido University for financial support. Partial support from the Cooperative Research Program of 'Network Joint Research Center for Materials and Devices' to TY and MM is gratefully acknowledged. YCL thanks Hokkaido University for the support for his stay in Sapporo.

References

1 H. Shirai, M. T. Nguyen, Y. Ishida and T. Yonezawa, *J. Mater. Chem. C*, 2016, **4**, 2228–2234.
2 C. Kim, G. Lee, C. Rhee and M. Lee, *Nanoscale*, 2015, **7**, 6627–6635.
3 J. K. Jiang, B. Bao, M. Z. Li, J. Z. Sun, C. Zhang, Y. Li, F. Y. Li, X. Yao and Y. L. Song, *Adv. Mater.*, 2016, **28**, 1420–1426.
4 L. Zhou, H. Y. Xiang, S. Shen, Y. Q. Li, J. D. Chen, H. J. Xie, I. A. Goldthorpe, L. S. Chen, S. T. Lee and J. X. Tang, *ACS Nano*, 2014, **8**, 12796–12805.
5 V. Sanchez-Romaguera, S. Wünscher, B. M. Turki, R. Abbel, S. Barbosa, D. J. Tate, D. Oyeka, J. C. Batchelor, E. A. Parker, U. S. Schubert and S. G. Yeates, *J. Mater. Chem. C*, 2015, **3**, 2132–2140.
6 Y.-C. Liao and Z.-K. Kao, *ACS Appl. Mater. Interfaces*, 2012, **4**, 5109–5113.
7 H. Lu, J. Lin, N. Wu, S. Nie, Q. Luo, C.-Q. Ma and Z. Cui, *Appl. Phys. Lett.*, 2015, **106**, 093302.
8 M. B. Gawande, A. Goswami, F.-X. Felpin, T. Asefa, X. Huang, R. Silva, X. Zou, R. Zboril and R. S. Varma, *Chem. Rev.*, 2016, **116**, 3722–3811.
9 Y. Yong, T. Yonezawa, M. Matsubara and H. Tsukamoto, *J. Mater. Chem. C*, 2015, **3**, 5890–5895.
10 T. Yonezawa, H. Tsukamoto and M. Matsubara, *RSC Adv.*, 2015, **5**, 61290–61297.
11 Y. Zhang, P. Zhu, G. Li, T. Zhao, X. Fu, R. Sun, F. Zhou and C. Wong, *ACS Appl. Mater. Interfaces*, 2014, **6**, 560–567.
12 Y. Hokita, M. Kanzaki, T. Sugiyama, R. Arakawa and H. Kawasaki, *ACS Appl. Mater. Interfaces*, 2015, **7**, 19382–19389.
13 T. Sugiyama, M. Kanzaki, R. Arakawa and H. Kawasaki, *J. Mater. Sci.: Mater. Electron.*, 2016, **27**, 7540–7547.
14 Y. Farraj, M. Grouchko and S. Magdassi, *Chem. Commun.*, 2015, **51**, 1587–1590.
15 T. Yonezawa, H. Tsukamoto, Y. Yong, M. T. Nguyen and M. Matsubara, *RSC Adv.*, 2016, **6**, 12048–12052.
16 A. Yabuki and S. Tanaka, *Mater. Res. Bull.*, 2012, **47**, 4107–4111.
17 M. Joo, B. Lee, S. Jeong and M. Lee, *Thin Solid Films*, 2012, **520**, 2878–2883.
18 H. Min, B. Lee, S. Jeong and M. Lee, *Opt. Lasers Eng.*, 2016, **80**, 12–16.
19 G. Qin, A. Watanabe, H. Tsukamoto and T. Yonezawa, *Jpn. J. Appl. Phys.*, 2014, **53**, 096501.
20 T. Araki, T. Sugahara, J. Jiu, S. Nagao, M. Nogi, H. Koga, H. Uchida, K. Shinozaki and K. Suganuma, *Langmuir*, 2013, **29**, 11192–11197.

 This journal is © The Royal Society of Chemistry 2017

Open Access Article. Published on 29 November 2016. Downloaded on 20/04/2017 06:52:53.
This article is licensed under a Creative Commons Attribution 3.0 Unported Licence.

21 H. Kang, E. Sowade and R. R. Baumann, *ACS Appl. Mater. Interfaces*, 2014, **6**, 1682–1687.
22 S.-J. Oh, Y. Jo, E. J. Lee, S. S. Lee, Y. H. Kang, H.-J. Jeon, S. Y. Cho, J.-S. Park, Y.-H. Seo, B.-H. Ryu, Y. Choi and S. Jeong, *Nanoscale*, 2015, **7**, 3997–4004.
23 Y.-T. Hwang, W.-H. Chung, Y.-R. Jang and H.-S. Kim, *ACS Appl. Mater. Interfaces*, 2016, **8**, 8591–8599.
24 Y.-H. Choi and S.-H. Hong, *Langmuir*, 2015, **31**, 8101–8110.
25 D.-H. Shin, S. Woo, H. Yem, M. Cha, S. Cho, M. Kang, S. Jeong, Y. Kim, K. Kang and Y. Piao, *ACS Appl. Mater. Interfaces*, 2014, **6**, 3312–3319.
26 S. J. Kim, J. Lee, Y.-H. Choi, D.-H. Yeon and Y. Byun, *Thin Solid Films*, 2012, **520**, 2731–2734.
27 W. Li, J. Jiu, S. Nagao and K. Suganuma, *J. Mater. Chem. C*, 2016, **4**, 8802–8809.
28 S. Magdassi, M. Grouchko, O. Berezin and A. Kamyshny, *ACS Nano*, 2010, **4**, 1943–1948.
29 Y. Long, J. Wu, H. Wang, X. Zhang, N. Zhao and J. Xu, *J. Mater. Chem.*, 2011, **21**, 4875–4881.
30 M. Grouchko, A. Kamyshny, C. F. Mihailescu, D. F. Anghel and S. Magdassi, *ACS Nano*, 2011, **5**, 3354–3359.
31 M. Matsubara, T. Yonezawa, T. Minoshima, H. Tsukamoto, Y. Yong, Y. Ishida, M. T. Nguyen, H. Tanaka, K. Okamoto and T. Osaka, *RSC Adv.*, 2015, **5**, 102904.
32 S. Jeong, S. H. Lee, Y. Jo, S. S. Lee, Y.-H. Seo, B. W. Ahn, G. Kim, G.-E. Jang, J.-U. Park and B.-H. Ryu, *J. Mater. Chem. C*, 2013, **1**, 2704–2710.
33 R. Guan, H. Hashimoto and K. H. Kuo, *Acta Crystallogr., Sect. B: Struct. Sci.*, 1984, **40**, 560–566.
34 R. Guan, H. Hashimoto and K. H. Kuo, *Acta Crystallogr., Sect. B: Struct. Sci.*, 1985, **41**, 219–225.
35 T. Yonezawa, Y. Uchida and H. Tsukamoto, *Phys. Chem. Chem. Phys.*, 2015, **17**, 32511–32516.
36 B. Faust, *Modern Chemical Techniques: An Essential Reference for Students and Teachers*, Royal Society of Chemistry, 1997.
37 X. H. Li, Y. Z. Meng, Q. Zhu and S. C. Tjong, *Polym. Degrad. Stab.*, 2003, **81**, 157–165.
38 S. Lin, W. Yu, X. Wang and C. Zhou, *Ind. Eng. Chem. Res.*, 2014, **53**, 18411–18419.
39 K. Nakano, S. Hashimoto, M. Nakamura, T. Kamada and K. Nozaki, *Angew. Chem., Int. Ed.*, 2011, **50**, 4868–4871.
40 X. Zhong, Z. Lu, P. Valtchev, H. Wei, H. Zreiqat and F. Dehghani, *Colloids Surf., B*, 2012, **93**, 75–84.
41 C. Yang, C. P. Wong and M. M. Yuen, *J. Mater. Chem. C*, 2013, **1**, 4052–4069.
42 B. H. Stuart, *Infrared Spectroscopy: Fundamentals and Applications*, John Sons, Ltd, Chichester, UK, 2004.